J Mater Sci (2011) 46:6096–6105
DOI 10.1007/s10853-011-5573-x

Improved optical and electrical response in metal–polymer nanocomposites for photovoltaic applications

V. Chaudhary · A. K. Thakur · A. K. Bhowmick

Received: 1 March 2011 / Accepted: 18 April 2011 / Published online: 3 May 2011

Abstract Hybrid nanocomposites based on polyethylene glycol (PEG) embedded with nanoscopic Ag particles were prepared by two distinct approaches: in situ and ex situ chemical processing routes. The effect of Ag loading on tailored optical and electrical responses in the two classes of metal–polymer nanocomposites (MPNs) was investigated. Transmission electron microscopy of the in situ MPN sample revealed core–shell-type combination comprising Ag nanoparticles lying at the core surrounded by polymeric (PEG) shell. On the other hand, ex situ MPNs exhibited dispersed phase microstructure with uneven distribution of Ag nanoparticles in the PEG matrix. Comparison of the thermal properties of in situ and ex situ MPNs confirmed that the MPN obtained through in situ process with 2 wt% of Ag contents displayed higher thermal stability ($\approx$18%) relative to ex situ MPN of the same composition. The absorption spectrum confirmed clear, blue shift with enhanced band gap in the case of in situ MPN relative to its ex situ counterpart. The Ag–PEG nanocomposites prepared by both the processes exhibited metallic I–V response. Electrical transport observed in terms of resistivity variation with temperature confirmed typical semiconducting behavior in the composite phase in sharp contrast to the insulating property of the host PEG. A large decrease ($\approx$65%) in activation energy was observed in the case of in situ MPN at higher loading of Ag possibly because of the higher mobility assisted by tunneling of charge carriers through polymeric spacers in the composite phase. The drastic improvement in optical and electrical responses of the nanocomposites indicated the suitability for photovoltaic and optoelectronic applications.

V. Chaudhary · A. K. Bhowmick (✉)
Department of Chemistry, Indian Institute of Technology Patna, Patna 800013, India
e-mail: director@iitp.ac.in; anilkb@rtc.iitkgp.ernet.in

A. K. Thakur
Department of Physics, Indian Institute of Technology Patna, Patna 800013, India

Introduction

Functional materials for energy storage/conversion devices have attracted significant attention in recent years. Metal oxide heterostructures, dye-sensitized polymers, ion-conducting polymers, etc. have emerged as important class of materials for applications in energy storage devices [1–4]. Metal–polymer nanocomposites are one such class having advantageous features of both the metallic and polymeric components. Dispersion of metal nanoparticles in soft polymeric matrix is expected to impart functional characteristics (electronic, optical, catalytic etc.) for specific tailored applications.

The origin of property tailoring in a metal–polymer nanocomposite system lies in the synergism between the properties of the individual components. It is well known that polymers act as the excellent host materials for metal as well semiconductor nanoparticles. When metal nanoparticles are embedded in a polymer, it surrounds and protects the metal nanoparticles from agglomeration and ensures nanoscopic features of the metallic filler in the composite phase [5–7]. Polyethylene glycol (PEG) is considered as a good host material for metal nanoparticles due to its specific features of low molecular weight, low Tg, water solubility and biocompatible properties that render it useful for industrial and biomedical applications [6, 8, 9]. At the same time, incorporation of metal

nanoparticles into a matrix improves its physical and chemical properties to a desirable level on composite formation. Among the metal nanoparticles, Ag nanoparticles have been studied due to its proven potential for applications in technologically important areas, such as photovoltaics, optoelectronics, energy storage, catalysis, sensing, high-energy radiation-shielding materials, microwave absorbers, optical limiters, polarizers, capacitors, actuating system, and biomedical materials [10–19].

The above mentioned specific applications require tunable properties in metal–polymer nanocomposites. Such a requirement can be achieved by lowering the nanoparticle size, ensuring homogeneity in size distribution and isotropy in morphology of the composite phase. Therefore, the control of these parameters of the metallic nanoparticles becomes a very challenging aspect. Further, dispersion and interfacial interactions of all the components in nanocomposites also influence the performance of these materials for wide ranging applications [20–25]. In addition, processing method of polymer-based hybrid nanocomposites also plays a crucial role in the control of composite stoichiometry and functional characteristics in the composite phase. Several approaches have been tried to ensure retention of nanoscale characteristics in the hybrid nanocomposites. Nevertheless, the in situ approach is still an attractive and less explored area.

Among the various methods for preparation of the metal–polymer nanocomposites, two are important and commonly used. The first is ex situ approach, in which direct mixing of metal nanoparticles with a polymer in solution phase is preferred. The other method is in situ formation of metal nanoparticles from metal precursors. In the in situ approach, the reaction occurs in the presence of a polymer, which ensures control over the size of the particles [5, 6, 26]. Some recent reports on metal–polymer nanocomposites have drawn considerable attention on their potential applications in view of their improved optical, mechanical, and thermal properties [27–31].

This article aims to report polymer–metal hybrid nanocomposite based on nano Ag-polyethylene glycol (PEG) combination. The control over particle size of Ag nanoparticles and their distribution in PEG matrix has been achieved via in situ chemical process. For the sake of comparison, the same composite has also been prepared via ex situ method. Physical characterization of Ag–PEG nanocomposite has been done using UV–Visible spectroscopy, transmission electron microscopy, and IR spectra. Thermal stability, voltage stability, and electrical property have been studied and analyzed. The suitability of the composite combination, prepared by both the approaches, has been investigated, and compared. This is a part of ongoing studies on polymer nanocomposites in this laboratory [32–37].

Experimental details

Reagents

All the chemicals were of analytic grade and used as received. Deionized water was used for the preparation of all the samples. Polyethylene glycol ($M_w = 3350$ g mol^{-1}) and silver nitrate were procured from Aldrich, India. Sodium citrate was purchased from Merck, India.

Materials preparation

Ag–PEG nanocomposites were prepared by two different processes, namely in situ and ex situ.

Synthesis of Ag–PEG nanocomposites by In situ process

Ag–PEG nanocomposites were prepared through in situ method by adding various amounts of silver nitrate to the solution of PEG before the addition of sodium citrate. In a typical experiment, PEG (0.5 g) was dissolved in deionized water (25 ml). 50 ml aqueous solution of silver nitrate was prepared and added to the PEG solution. The resulting mixture solution was boiled for about 15 min with continuous stirring. 25 ml aqueous solution of sodium citrate (5.88×10^{-4} M) was prepared separately and added dropwise into the above reaction mixture with the help of a dropper. The final solution was kept again for boiling with continuous stirring for about 30 min. The color of the solution became pale yellow. The resulting colloidal solution was then cooled down slowly at room temperature and finally stored at 5 °C. For the optimization of these nanocomposites through this method, we varied the amount of Ag content with fixed amount of PEG. The best results were obtained with 2 wt% of Ag.

Synthesis of Ag–PEG nanocomposites by ex situ process

For the synthesis of Ag–PEG nanocomposites through ex situ method, preparation of nanocomposites was carried out into two parts. First, the colloidal silver nanoparticles of various concentrations were prepared by the reduction of silver ions using sodium citrate via steps as reported in the literature [38] with some modification. Initially, 25 ml of sodium citrate of 5.88×10^{-4} M was added dropwise into 50-ml-boiled silver nitrate solution with continuous stirring. The resulting mixture was then refluxed for about 30 min with continuous stirring. Finally, yellow-colored Ag nanoparticles were obtained. It was allowed to cool down at room temperature. Next, 25 ml aqueous solution of PEG was prepared separately and added into colloidal solution of the as-prepared Ag nanoparticles at room temperature with continuous stirring for about 30 min.

These nanocomposites were also optimized by varying the amount of Ag content with fixed amount of PEG.

Materials characterization

Transmission electron microscopy (TEM)

Transmission electron microscopy was performed on a FEI-Philips Morgagni 268D Digital TEM with image analysis system by applying an accelerating voltage of 100 kV. Transmission electron micrographs of different samples were recorded by applying a small drop of colloidal solution into the carbon-coated copper G-200 grid. Copper grid was dried in dark before its examination. The particle size was analyzed using "Analysis 3.2" "soft imaging system" SIS Olympus.

Thermogravimetric analysis (TGA)

Thermogravimetric analyses of pure PEG and metal–polymer nanocomposites (MPNs) were carried out on a Perkin Elmer TGA instrument [Model: Pyris Diamond TG/DTA] and TA instrument [Model: SDT Q600]. The measurements were performed from the ambient temperature to 600 °C with heating rate of 20 °C/min under nitrogen atmosphere.

Fourier transform infrared spectroscopy (FTIR)

The FTIR spectra of all the samples were measured using a Perkin Elmer FTIR-spectrophotometer (Model RX-1), within the range of 400–4400 cm^{-1} using a resolution of 4 cm^{-1} in KBr medium.

UV–Vis spectroscopy

The UV–Visible spectra of pure PEG and Ag–PEG nanocomposites were recorded using a Systronic Spectrophotometer (Model 2203). These spectra were generally recorded in a 1 cm quartz cell.

I–V Characteristics

The current–voltage (I–V) characteristics of pure PEG and the MPNs were determined with using digital picoammeter (scientific equipment, model DPA—111) and power source (ELNOVA). A voltage step of 0.5 V and preset relaxation time of 5 s were used in all the cases. The voltage sweeps were recorded ranging from −10 to +10 V range. For the measurement of I–V characteristics, the samples were solidified by using rotaevaporator and then dried in desiccator for 2–3 days. The solid samples were cold pressed into cylindrical pellets of diameter of 10 mm and pellet thickness in the 2–3 mm range for different Ag nanofiller concentrations. The pellets were finally coated with conductive carbon paint and dried at room temperature for 3 h before carrying out the measurements.

Electrical conductivity measurements

The electrical conductivity measurements of pure PEG and all MPNs were carried out at an input ac signal level ~1.2 V peak to peak over a temperature range of 30–55 °C using a computer-controlled impedance analyzer (HIOKI LCR Hi TESTER, Model: 3532) in the frequency range of 100 Hz–100 kHz.

Results and discussion

Transmission electron microscopy

The TEM micrographs of MPNs prepared by in situ and ex situ processes are shown in Fig. 1a–c. TEM image analysis provides visual evidence for distinctly different morphological features of the Ag–PEG nanocomposites obtained via in situ and ex situ processing routes in the present study. An observation of these images reveals that the in situ MPN sample having 2 wt% of Ag consists of non-aggregated, scattered, and spherical silver nanoparticles. From the TEM image of this sample, the average size of the particles is determined to be 15 nm with a size distribution of 9–22 nm (Fig. 1a) and indicates the presence of nanoscopic Ag imbedded in the PEG matrix in the form of core–shell-type geometry (Inset of Fig. 1a). Well-resolved Ag nanoparticles lying at the core appear to be surrounded by polymeric shell, thereby confirming formation of core–shell-type nanoscopic composite structure.

On the other hand, Ag–PEG nanocomposites prepared via ex situ process provide clear evidence of Ag nanoparticle agglomeration in the PEG matrix. Clustering of the Ag nanofiller revealed in TEM micrograph for 2 wt% of Ag dispersed composite provides convincing evidence in support of our interpretation (Fig. 1b). It may be attributed to surface interaction among Ag nanoparticles because of their high surface area and small particle size (27 nm). This has been confirmed by an increase in the size of cluster on increasing the Ag nanoparticle loading (≈4 wt%) in the PEG matrix (Fig. 1c). The dispersed agglomerates of Ag nanoparticles get converted into localized clusters of larger size with increased Ag nanoparticle loading in the PEG.

Thermogravimetric analysis

Figure 2 shows the TGA thermograms depicting weight loss as a function of temperature of in situ and ex situ

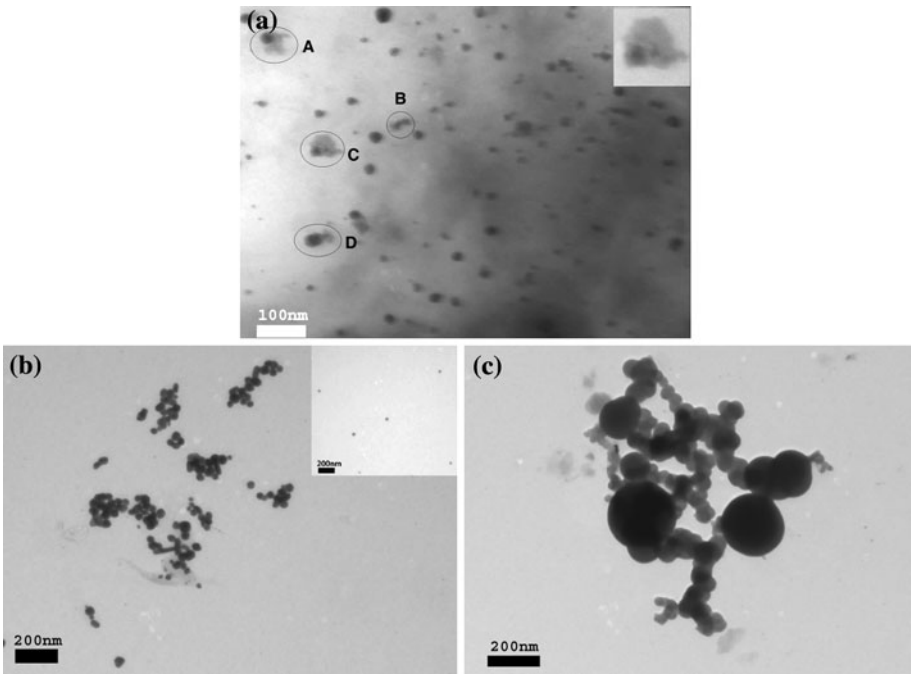

Fig. 1 TEM images of Ag–PEG nanocomposites: In situ sample having 2 wt% of Ag (**a**), Ex situ sample having 2 wt% of Ag (**b**), and 4 wt% of Ag (**c**). Inset of Fig. 1a shows the enlargement of *circle* region C, representing the core–shell-type structure, and the inset of Fig. 1b shows the image of pure Ag nanoparticles

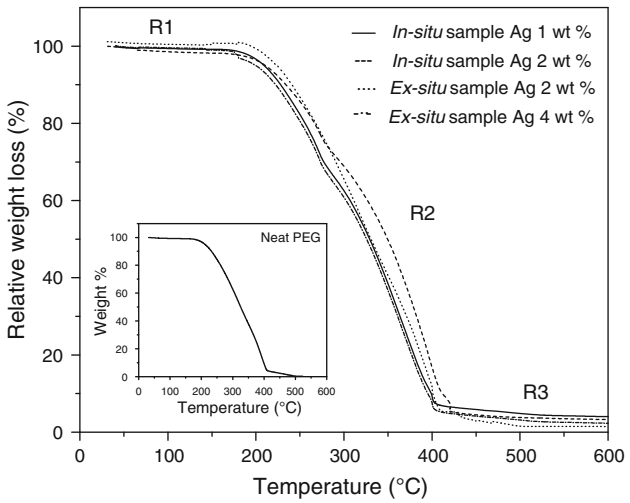

Fig. 2 TGA thermogram of Ag–PEG nanocomposites of in situ and ex situ samples having different wt% of Ag. Inset shows the TGA thermogram of neat PEG

samples of Ag–PEG nanocomposites and neat PEG measured under nitrogen atmosphere. The TGA curves of neat PEG and Ag–PEG nanocomposites can be divided into three regions: (i) a very slowly varying flat region (R1, <200 °C). This region indicates initially loss in weight, which is identical for all the samples. It may possibly be due to the release of surface moisture; (ii) a sharp fall in weight indicated by R2 region (200 °C < T < 400 °C); and (iii) a flat R3 region (>400 °C). In this R3 region, neat PEG undergoes complete thermal decomposition because of chain scission at $T \geq 400$ °C. However, a clear, though marginal, improvement is noted for Ag–PEG nanocomposites with

Table 1 TGA data of Ag–PEG nanocomposites with various contents of Ag

Samples	Degradation onset temperature (°C)	Decomposition temperature (°C)
Pure PEG	241	408
In situ sample Ag 1 wt%	249	406
In situ sample Ag 2 wt%	296	420
Ex situ sample Ag 2 wt%	251	409
Ex situ sample Ag 4 wt%	236	402

leftover residue. This may be related to Ag contents in the PEG matrix. R2 region indicates that the thermal degradation is a typical feature both for neat PEG and Ag–PEG nanocomposites. Onset of degradation occurs at 241 °C for neat PEG, and at 249 and 296 °C for 1 and 2 wt% of Ag loadings MPN, respectively, obtained via in situ process. In the case of ex situ samples, onset of degradation occurs at 251 and 236 °C for 2 and 4 wt% of Ag, respectively (Table 1). These results exhibit a clear improvement in thermal stability in terms of enhancement in the onset of decomposition on Ag dispersion in PEG matrix. However, the processing methodology used in the composite formation (in situ and ex situ) has distinctly different thermal stability level. The Ag–PEG nanocomposites formed by the in situ method with 2 wt% of Ag contents are 23% more stable than PEG (Inset of Fig. 2). These nanocomposites formed by the ex situ method with the same composition are 4% more stable than PEG, the host polymer. A comparison suggests that composites of Ag–PEG obtained via in situ

process have higher thermal stability ($\approx$ by 18%) than ex situ composite of the same composition. A relative comparison of the stability features is presented in the Table 1.

FTIR spectra

The FTIR spectra of neat PEG and Ag–PEG nanocomposites having different wt% of Ag are shown in Fig. 3. The spectrum of the neat PEG showed many characteristic bands of molecular groups constituting the host polymer, PEG. They have been identified and assigned as shown in Table 2. In the spectrum of the neat PEG, bands around 950, 1105 and 2879 cm^{-1} correspond to –CH out-of-plane bending vibration, C–O–C group stretching, and $–CH_2$ stretching, respectively.

An analysis of the Ag–PEG nanocomposites prepared by in situ process (in situ sample) having 1 and 2 wt% loading of Ag shows that the bands pertaining to C–OH, C–O–C, and CH_2 are affected (Fig. 3a). From the IR spectra of these samples, it is evident that the band attributed to $\nu(CH_2–$ breathing mode) exhibits downward shift at 1 wt% of Ag and an upward shift at 2 wt% of Ag (Table 2). However, C–O–C band exhibits a noticeable change, i.e., an upward shift only at 2 wt% of Ag loading in the composite phase (Fig. 3b, Table 2).

On the other hand, in the Ag–PEG nanocomposites prepared by ex situ process (ex situ sample), splitting in the vibrational bands attributed to ν(–CH) and ν(C–O–C) takes place (Fig. 3c). The result suggests the possibility of strong interaction of Ag with polymer backbone. It may be due to

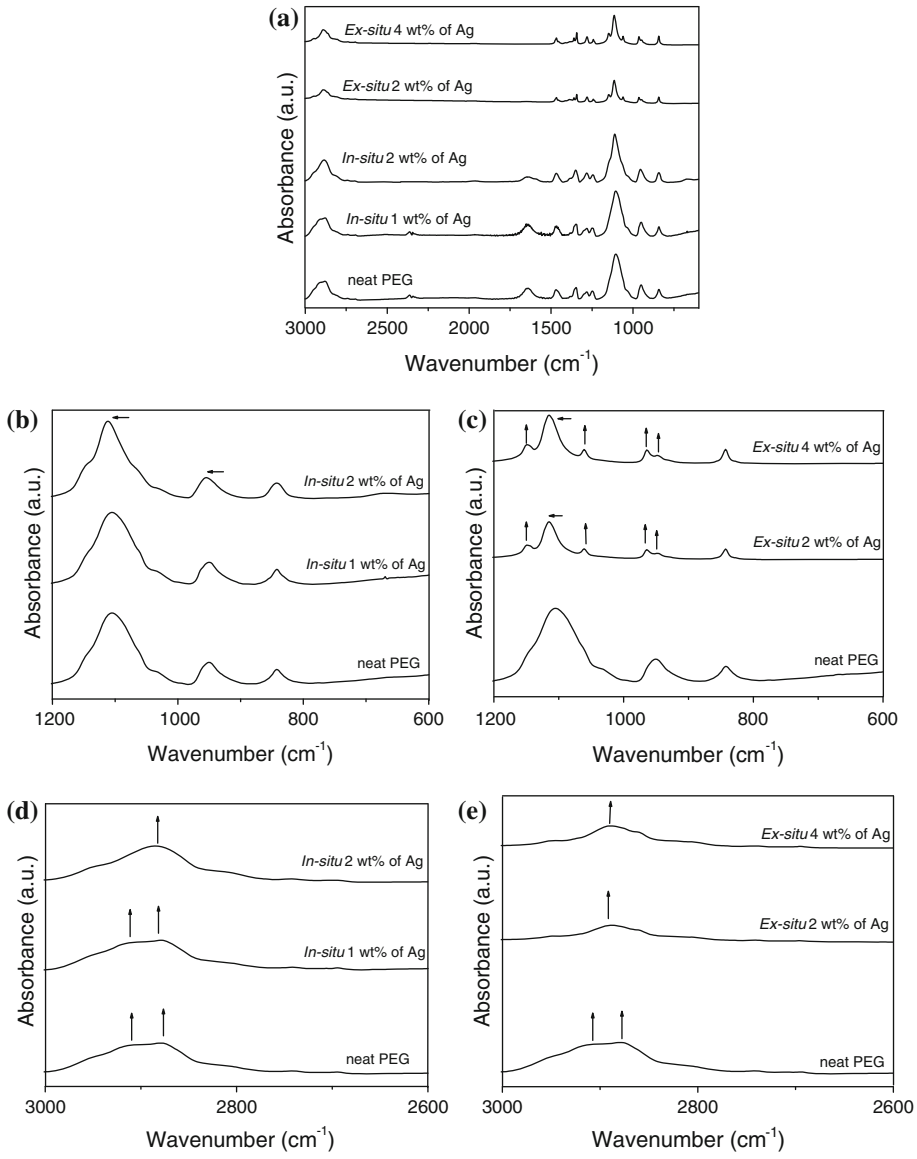

Fig. 3 FTIR spectra of neat PEG and Ag–PEG nanocomposites having different wt% of Ag in different ranges. 3000–600 cm^{-1} (**a**); 1200–600 cm^{-1} (**b**, **c**); and 3000–2600 cm^{-1} (**d**, **e**)

Table 2 FTIR spectral data (cm^{-1}) of pure PEG and Ag–PEG nanocomposites

Metal–polymer Nanocomposite (MPN) sample composition		FTIR band positions				
		Band assignment				
		–CH out-of-plane bending	C–OH stretching	C–O–C stretching	CH_2 breathing	CH_2 stretching
Host polymer PEG		950	1033	1105	1348	2879
In situ MPN	1 wt% of Ag	948	1033	1105	1344	2879
	2 wt% of Ag	954	1037	1112	1350	2885
Ex situ MPN	1 wt% of Ag	950	1060	1113	1343	2889
	2 wt% of Ag	947	1060	1114	1343	2889
	3 wt% of Ag	947	1060	1115	1343	2889
	4 wt% of Ag	947	1060	1114	1343	2889

Lewis acid–base-type interaction between the nanofiller and host polymer.

Feasibility of (C–O$^{\cdot\cdot}$H–Ag) and (C–O$^{\cdot\cdot}$–C–Ag) interactions has been evident by their upward shift. Further, an upward shift of the host polymer (PEG) FTIR bands—1033 cm^{-1} (attributed to ν(C–OH)) and 1105 cm^{-1} (attributed to ν(C–O–C))—on the nano-Ag loading suggests the possibility of stronger interaction between active metal surface and electron-rich sites of the polymer backbone (Table 2). In addition, a shift of 2879 cm^{-1} band toward the higher side both in the in situ and ex situ composites suggests a clear evidence for stabilization and strengthening of the polymer backbone on interaction with nano-Ag in the composite phase. Such an interaction between nanocrystalline Ag and electron rich O$^{\cdot\cdot}$—atom in the PEG matrix of the MPN seems analogous to the dπ–pπ-type interaction in the metal–ligand combination in inorganic complexes.

From the analysis of the FTIR spectra in the region of 3000–2600 cm^{-1} of in situ and ex situ samples having 2 wt% of Ag, it is observed that the vibration stretching frequency due to CH_2 group is shifted to 2885 and 2889 cm^{-1} for in situ and ex situ MPNs, respectively. This shift is also accompanied by a change in band profile (position, size, and shape) of the vibrational band (Fig. 3d–e, Table 2).

A comparison of the FTIR spectra of Ag–PEG nanocomposites prepared via two different processes clearly suggests two distinct mechanism of composite formation. The former may be attributed to core–shell-type composite, whereas the latter may be related to dispersed phase composite. It is because the in situ MPN sample has shown surface interaction between the host polymer and filler as if there is a core–shell-type structure. It has exhibited limited ability of the filler acceptability beyond which phase separation occurs. Such a possibility also seems logical and convincing as revealed in TEM micrograph.

Therefore, an analysis of FTIR spectra of Ag–PEG nanocomposites prepared using different methodology with same composition of Ag shows different pattern of band shifting. These results exhibit that the PEG chains are immobilized at the surface of Ag nanoparticles because of strong interactions. These interactions may be due to the presence of non-covalent interactions (hydrophobic/van der Waals/electrostatic) between Ag nanoparticles and different PEG molecules.

UV–Visible spectra

Figure 4a presents the absorption spectra of neat PEG and Ag–PEG nanocomposites prepared via in situ and ex situ processes. A comparison indicates that Ag–PEG nanocomposites exhibit strong absorption maxima, the position of which varies depending on the process conditions and loading level of Ag nanoparticles in the composite phase. The absorption peak, on the other hand, could not be noticed for neat PEG. The well-defined single, broad and asymmetric absorption maxima, occurring at $\sim$415 nm (for 1 wt% Ag) and 425 nm (for 2 wt% Ag) in the in situ samples, and at 427 nm (for 2 wt% Ag), and 430 nm (for 4 wt% Ag) in the case of ex situ process-based MPNs, may be related to the presence of "surface plasmon resonance" phenomena of Ag nanoparticles. This is a characteristic feature of noble metal nanoparticles, such as nano-Ag, near their conduction bands.

A relative analysis of the MPNs indicates that the absorption spectrum is sharper in the case of in situ process-based MPNs in comparison to that of the ex situ process obtained MPN sample. This change may be attributed to the homogeneity and isotropy of the nanoscopic metal (Ag) particle size distribution in the composite phase. Another point to be noted is the observed red-shift in the absorption spectrum that depends predominantly on the weight fraction of the nano-Ag in the MPN. Such an effect tailors the refractive index of the metal–polymer nanocomposite and affects the "band gap" of the MPNs.

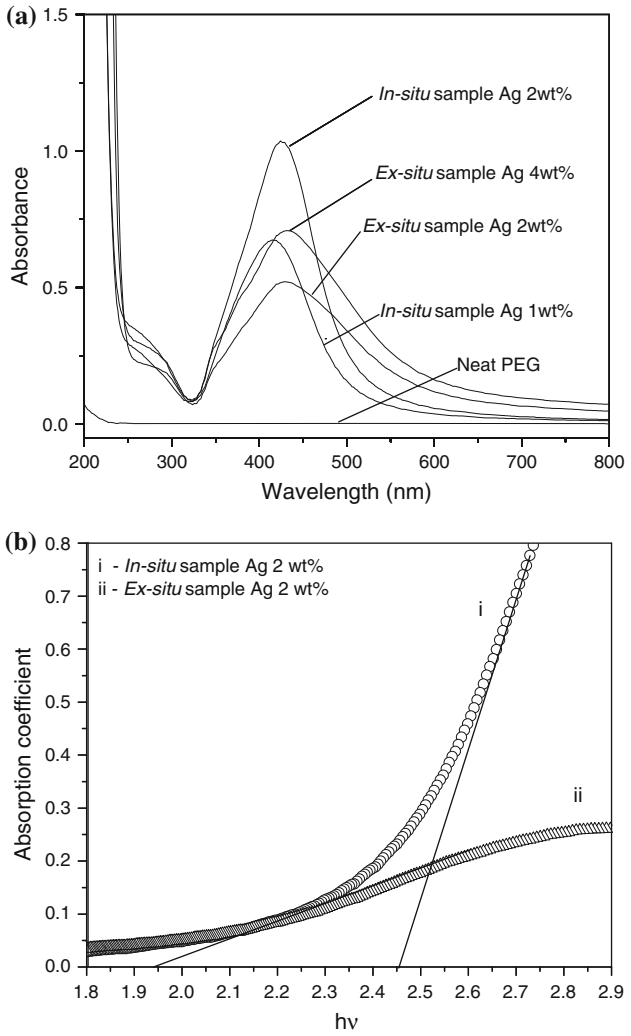

Fig. 4 UV–Visible spectra (**a**) of neat PEG and Ag–PEG nanocomposites of in situ and ex situ samples having different wt% of Ag and band gap calculation spectra for 2 wt% of Ag (**b**)

Table 3 Band gap information of Ag–PEG nanocomposites

Samples	Estimated band gap (eV)
In situ sample Ag 1 wt%	2.41
In situ sample Ag 2 wt%	2.46
Ex situ sample Ag 2 wt%	1.94
Ex situ sample Ag 4 wt%	1.97

The band gap of the MPNs has been estimated using the relation:

$$\alpha h\nu = \sqrt{A}\left(h\nu - E_g\right) \quad (1)$$

where, E_g is band gap, and α = absorption coefficient = A/d, where A = I/I_0 = absorbance, and d = film thickness. The estimated band gap is compared in Table 3 for the MPN obtained via the in situ and ex situ processes. The results indicate a relatively higher band gap for the MPN obtained via the in situ process than that in the ex situ MPN. This is also shown in Fig. 4b for comparison.

Current–Voltage (I–V) characteristics

Figure 5a–b shows I–V Characteristics of Ag–PEG nanocomposites obtained by in situ and ex situ processes. A preliminary comparison of the result clearly suggests drastic difference in the I–V response of the Ag–PEG nanocomposites obtained via both the routes. The results indicate that neat PEG is nonresponsive to the applied dc bias up to 10 V. However, this behavior, attributed primarily to the insulating property of PEG, changes drastically on composite formation with Ag nanoparticles.

Figure 5a (ii, iii) represents I–V response of Ag–PEG nanocomposites obtained by the in situ process. It exhibits typical linear response for composites with 1 and 2 wt% of Ag with an essential difference in their stability window on voltage scale. In situ nanocomposite with 1 wt% of Ag shows relatively lower current and wider voltage stability limit than the composite sample with 2 wt% of Ag. In the latter, current begins to rise at voltage (V) $\geq \pm$ 2 V and increases linearly up to 7 V. Beyond this voltage, current attains an optimum threshold limit suggesting possibility of breakdown. The values of current drawn at different voltages are given in Table 4.

On the other hand, I–V responses of ex situ nanocomposites are distinctly different in terms of voltage stability window irrespective of Ag nanoparticle loading fraction in the PEG matrix. The typical response, however, remains linear (ohmic). The difference in I–V response may be due to conduction behavior in both the types of composites in sharp contrast to that of the neat PEG. Hence, the MPN based on nano-Ag in the PEG exhibits metallic response, indicated by I–V characteristics. However, the band gap estimates (Table 3) suggest semiconducting behavior with larger band gap than that of the conventional intrinsic semiconductors (Ge, Si, etc.)[39].

Electrical transport property

The indications from UV–Visible and I–V characteristics prompted us to probe electrical transport properties of the MPNs. The variation of the resistivity as a function of temperature for different concentrations of Ag in both in situ and ex situ nanocomposites are shown in Fig. 6. The resistivity vs temperature pattern exhibits typical negative temperature coefficient of resistance (NTCR) behavior analogous to semiconductors. The absorption spectrum analysis has also confirmed this with a slightly higher band gap than that of the normal semiconductors.

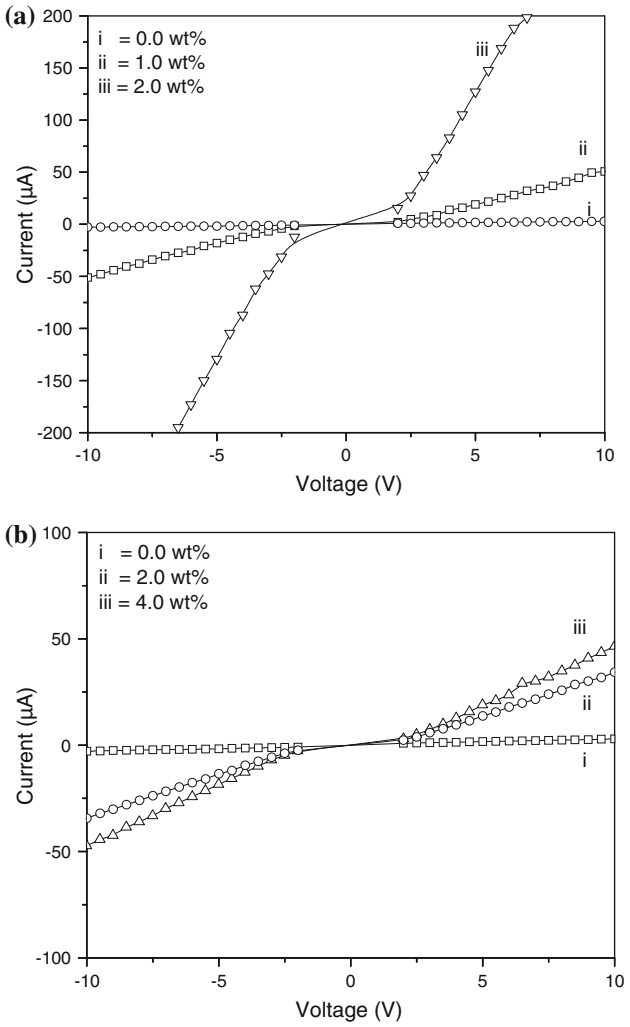

Fig. 5 I–V characteristics curves of neat PEG and Ag–PEG nanocomposites of in situ (**a**) and ex situ (**b**) samples having different wt% of Ag

The variations of the electrical conductivity (σ_{dc}) as a function of temperature for different concentrations of Ag in in situ and ex situ nanocomposites and neat PEG are shown in Fig. 7. Electrical conductivity provides information associated to transport of the charge carrier, i.e., electron/holes or cations/anions that predominate the

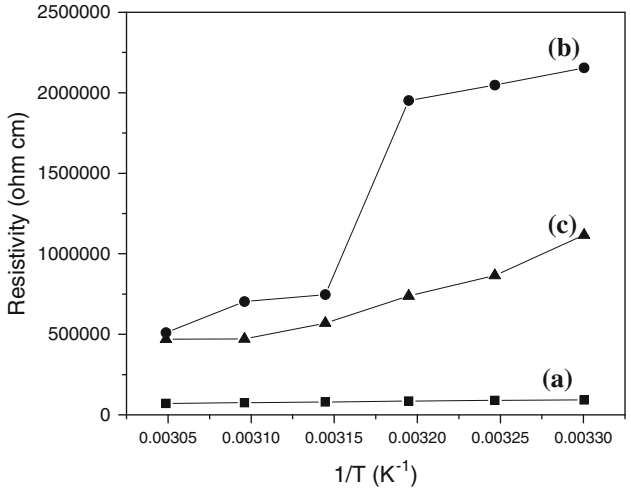

Fig. 6 Variation of the resistivity (ρ) of in situ sample of Ag–PEG nanocomposites having 2 wt% of Ag (**a**) and ex situ sample of Ag–PEG nanocomposites having 2 wt% of Ag (**b**) and 4 wt% of Ag (**c**) as a function of temperature

process of conduction. The pattern of the conductivity in all the curves of Fig. 7 indicates that σ_{dc} increases with increase in temperature irrespective of the type of MPN samples. The dependence of the electrical conductivity on temperature follows the Arrhenius relation:

$$\sigma = \sigma_0 \exp^{-Ea/KT} \quad (2)$$

where σ_0, E_a, T, and K are the pre exponential factor, activation energy, temperature, and Boltzmann constant, respectively. In both types of MPN samples (in situ and ex situ), the electrical conductivity shows a clear increase with an increase in temperature. A linear fit of σ_{dc} versus 10^3/T has been used to determine the activation energy. The corresponding values of activation energy for all the samples are recorded in Table 5. These results exhibit that the activation energy decreases with an increase in the contents of Ag in both types of samples but this decrease in activation energy is more prominent in in situ samples (with high content of Ag). This has happened possibly because of the higher mobility of charge carriers in in situ samples as compared with the ex situ samples.

Table 4 I–V characteristics of Ag–PEG nanocomposites

Sample	Current (μA) at selective voltage									
	−6 V	−5 V	−4 V	−3 V	−2 V	2 V	3 V	4 V	5 V	6 V
Neat PEG	−1.9	−1.7	−1.4	−1.1	−0.9	0.9	1.1	1.4	1.7	1.9
In situ sample Ag 1 wt%	−25.4	−18.1	12.2	−6.8	−1.5	2.1	7.2	13.7	19	25.1
In situ sample Ag 2 wt%	−173	−129.4	−87	−47.5	−12.2	15.3	47	83	127.1	168.7
Ex situ sample Ag 2 wt%	−17.6	−13.4	−9.4	−5.7	−2.4	2.45	5.9	9.5	13.7	17.9
Ex situ sample Ag 4 wt%	−24.3	18.5	−12.8	−7	−2.7	2.9	7.3	12.7	18.9	23.6

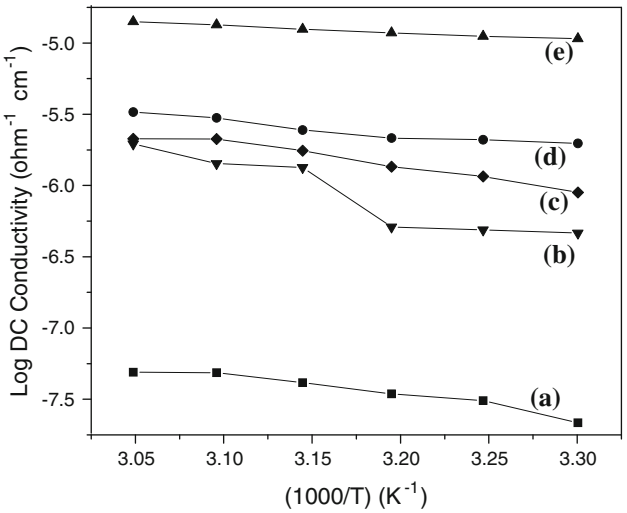

Fig. 7 Variation of the electrical conductivity (σ_{dc}) of neat PEG (**a**); ex situ samples of Ag–PEG nanocomposites (b = 2 wt% of Ag, c = 4 wt% of Ag) and in situ samples of Ag–PEG nanocomposites (d = 1 wt% of Ag, e = 2 wt% of Ag) as a function of the temperature for various concentrations of Ag

Table 5 Activation energy data of neat PEG and Ag–PEG nanocomposites with a temperature range 30–55 °C

Samples	Activation energy (eV)
Neat PEG	0.111
In situ sample Ag 1 wt%	0.079
In situ sample Ag 2 wt%	0.038
Ex situ sample Ag 2 wt%	0.239
Ex situ sample Ag 4 wt%	0.141

Conclusions

Metal–polymer nanocomposites (MPNs) obtained via in situ and ex situ chemical processes have been prepared over a feasible range of compositions. The MPNs have been analyzed for the role of nanoscopic metal on changes in stability (thermal, voltage, etc.), microstructure, electrical transport, and optical properties. In situ MPN has shown core–shell-type structure. On the other hand, ex situ MPNs have exhibited typical dispersed phase composite microstructutre with certain degree of inhomogeneity in the dispersion of nano-Ag in the PEG matrix. The experimental results indicate that an insulating host polymer (PEG) has shown drastic change in its electrical and optical properties on nanocomposite formation. Although the MPN samples exhibit metallic I–V response, electrical transport and optical properties, noted in terms of resistivity variation with temperature and band gap estimates, confirmed typical semiconducting property with relatively higher band gap than the conventional semiconductors (Ge, Si etc.).

An overall comparison suggested that the in situ process-based nanocomposite has shown larger improvement in properties over its ex situ counterpart. However, both the MPNs appear to be lucrative for energy storage device (photovoltaic), radiation sensors, etc.

Acknowledgements The financial support of IIT Patna is gratefully acknowledged to enable the authors undertake this study. VC is thankful to the Director, IIT Patna, for providing the laboratory and instrumentation facilities. Thanks are also due to the Director, AIIMS, New Delhi for providing the facilities of TEM. Special thanks are also due to the co-workers of Prof A K Bhowmick, who are working in the Rubber Technology Centre, IIT Kharagpur, for their valuable cooperation during experiments. AKB is thankful to DST, New Delhi and Commonwealth of Australia for providing Indo-Australia Strategic Research Fund.

References

1. Chatterjee S (2008) J Mater Sci 43:1696. doi:10.1007/s10853-007-2376-1
2. Jager C, Bilke R, Heim M, Haarer D, Karickal H, Thelakkat M (2001) Synth Metals 121:1543
3. Karim SMA, Nomura R, Sanda F, Seki S, Watanabe M, Masuda T (2003) Macromolecules 36:4786
4. Pal K, Kang DJ, Zhang ZX, Kim JK (2010) Langmuir 26:3609
5. Nicolais L, Carotenuto G (2005) Metal-polymer nanocomposites. Johan Wiley & Sons, New Jersey
6. Ajayan PM, Schadler LS, Braun PV (2003) Nanocomposite science and technology. Wiley VCH Verlag, GmbH & Co. KGaA, Weinheim
7. Leventis HC, King SP, Sudlow A, Hill MS, Molloy KC, Haque SA (2010) Nano Lett 10:1253
8. Yuan Y-Y, Liu X-Q, Wang Y-C, Wang J (2009) Langmuir 23:2126
9. Chen Q, Yue L, Xie F, Zhou M, Fu Y, Zhang Y, Weng J (2008) J Phys Chem 112:10004
10. Kickelbick G (2003) Prog Polym Sci 28:83
11. Panigrahi S, Kundu S, Ghosh SK, Nath S, Pal T (2004) J Nanopart Res 6:411
12. Temgire MK, Joshi SS (2004) Rad Phys Chem 71:1039
13. Mukherjee B, Mukherjee M (2009) Appl Phys Lett 94:73510-1
14. Khanna PK, Singh N, Charan S, Subbarao VVVS, Gokhale R, Mulik UP (2005) Mater Chem Phys 93:117
15. Lu J, Moon K-S, Xu J, Wong CP (2006) J Mater Chem 16:1543. doi:10.1039/b514182f
16. Ohnuma A, Cho EC, Jiang M, Ohtani B, Xia Y (2009) Langmuir 25:13880
17. Rajesh, Ahuja T, Kumar D (2009) Sens Actuators B 136:275
18. Kim D, Park S, Lee JH, Jeong YY, Jon S (2007) J Am Chem Soc 129:7661
19. Khemtong C, Kessinger CW, Gao J (2009) Chem Commn 24:3497
20. Fu S-Y, Feng X-Q, Lauke B, Mai Y-W (2008) Compos Part B 39:933
21. Mayer ABR (1998) Mater Sci Eng C 6:155
22. Faupel F, Zaporojtchenko V, Strunskus T, Elbahri M (2010) Adv Eng Mater 112:1177
23. Pakula C, Zaporojtchenko V, Strunskus T, Herges R, Faupel F (2010) Nanotechnology 21:465201
24. Bernabo M, Pucci A, Ramanitra HH, Ruggeri G (2010) Materials 3:1461
25. Gupta K, Jana PC, Meikap AK (2010) Synth Metals 160:1566

26. Yu D-G, Lin W-C, Lin C-H, Chang L-M, Yang M-C (2007) Mater Chem Phys 101:93
27. Mukherjee S, Mukherjee M (2006) J Phys Condens Matter 18:11233
28. Datta H, Bhowmick AK, Singha NK (2009) Polymer 50:3259
29. Mbhele ZH, Salemane MG, Sittert CGCEV, Nedeljkovic JM, Djokovic V, Luyt AS (2003) Chem Mater 15:5019
30. Bai J, Li Y, Du J, Wang S, Zheng J, Yang Q, Chen X (2007) Mater Chem Phys 106:412
31. Gautam A, Ram S (2010) Mater Chem Phys 119:266
32. Sadhu S, Bhowmick AK (2005) J Mater Sci 40:1633–1642 10.1007/S10853-005-0663-2
33. Bandyopadhyay A, Sarkar MD, Bhowmick AK (2005) J Polym Sci Part B Polym Phys 43:2399
34. Kar S, Bhowmick AK (2009) J Nanosci Nanotechnol 9:3144
35. Ganguly A, Bhowmick AK (2008) Macromolecules 41:6246
36. Maiti M, Bhowmick AK (2009) J Appl Polym Sci 111:1094
37. Bhattacharya M, Bhowmick AK (2010) Rubber Chem Technol 83:16
38. Lee PC, Meisel D (1982) J Phys Chem 86:3391
39. Streetman B, Banerjee S (2000) Solid state electronic devices. Prentice Hall, New Jersey